INTERNATIONAL JOURNAL OF
NUMERICAL ANALYSIS AND MODELING
Volume 23, Number 4, Pages 461–479

doi: 10.4208/ijnam2026-1020

THE ENERGY STABLE SIXTH-ORDER IMPLICIT-EXPLICIT SCHEME WITH SCALAR AUXILIARY VARIABLE METHOD FOR THE SWIFT-HOHENBERG EQUATION

JUNDONG FENG, YUANYUAN KANG, AND YIN YANG*

Abstract. In the present work, we propose two kinds of sixth-order numerical scheme for the Swift-Hohenberg (SH) equation. We adopt the implicit-explicit sixth-order scheme (BDF6) combined with the generalized scalar auxiliary variable (GSAV) method for temporal discretization and the Fourier spectral approach for spatial discretization. We rigorously prove the energy dissipation law of our proposed scheme and the H^2 norm error analysis. Furthermore, we promote the corresponding numerical scheme with the exponential scalar auxiliary variable (ESAV) method, which satisfies energy dissipation law. Finally, we show the substantial examples that verify the energy dissipation property and convergence of the two schemes.

Key words. Swift-Hohenberg equation, BDF6 scheme, energy stability, GSAV method and ESAV method.

1. Introduction

The L^2 gradient flow models are remarkable for describing diverse phase transitions, with the Swift-Hohenberg (SH) equation [1] as a representative example. This model is extensively used to simulate complex physical phenomena, including interface dynamics, liquid crystals, and biological tissues [2, 3, 4, 5, 6, 7]. In this paper, we consider the SH equation and derive its governing equation as follows.

$$\phi_t = -\frac{\delta \mathcal{E}}{\delta \phi} = -\left(\Delta^2 \phi + 2\Delta\phi + f(\phi)\right), \tag{1}$$

$$\phi(\cdot, t) \text{ is } \Omega - \text{periodic}, \ t \in (0, T], \tag{2}$$

$$\phi(x, 0) = \phi_0(x), \ x \in \Omega, \tag{3}$$

where Ω is a bounded closed domain in $\mathbb{R}^d$ $(d = 1, 2, 3)$, $\phi(x, t)$ denotes density fields and the function $f(\phi) = \phi^3 - \beta\phi^2 + (1-\epsilon)\phi$, the parameters ϵ and β are nonnegative constants relating to physical properties and Δ is the Laplace operator. The energy functional is defined as

$$\mathcal{E}(\phi) = \int_\Omega \left[\frac{1}{2}(\Delta\phi)^2 - |\nabla\phi|^2 + \frac{1}{4}\phi^4 - \frac{\beta}{3}\phi^3 + \frac{1-\epsilon}{2}\phi^2\right] \mathrm{d}x.$$

Thus, it is evident that the energy functional is nonincreasing in time:

$$\frac{d\mathcal{E}}{dt} = \int_\Omega \frac{\delta \mathcal{E}}{\delta \phi}\phi_t \mathrm{d}x = -\int_\Omega \left(\frac{\delta \mathcal{E}}{\delta \phi}\right)^2 \mathrm{d}x \le 0.$$

The SH equation is a fourth-order nonlinear partial differential equation. Due to its high-order nonlinearity and parameter perturbations, finding analytical solutions is challenging. Therefore, establishing stable and efficient numerical algorithms is of great significance. In recent years, many scholars have conducted extensive numerical studies on the SH equation, with the energy dissipation property being regarded

Received by the editors on June 19, 2024 and accepted on October 30, 2025.
2000 *Mathematics Subject Classification.* 65M06, 65M12.

as a crucial criterion for evaluating the accuracy of numerical algorithms. For instance, Qi et al. [32] proposed the backward Euler scheme and the Crank-Nicolson (CN) scheme based on the invariant energy quadratization (IEQ) theory for the SH equation. Both schemes were shown to satisfy energy stability. Additionally, Hou et al. [34] developed a linear CN scheme with two stabilization terms for the SH equation. The authors provided a detailed proof demonstrating that the scheme is energy-stable and achieves second-order accuracy in time. Lee [12] employed the operator splitting method to construct first- and second-order Fourier spectral schemes. The author verified the energy stability of the schemes through numerical experiments. For other phase field models, Lee and Yoon [14] investigated the energy stability of the first-order convex splitting scheme. The models tested include the Allen-Cahn (AC), Cahn-Hilliard (CH), and molecular beam epitaxy (MBE) equations. In further research, Lee [31] proposed energy-stable first- and second-order numerical schemes for the SH equation based on the convex splitting method. Using the implicit-explicit Runge-Kutta (RK) method, Lee [15] developed first- to third-order linear numerical schemes for the SH equation, all of which satisfy mass conservation. Zhao et al. [19] investigated the BDF3 scheme of the SH equation, and provided the L^2 norm error analysis and the energy stability. Kang et al. [35] proposed the linear BDF2 scheme with a stabilization term for the MBE model without slope selection, using variable time step, and the authors proved its modified energy stability and convergence. Wang et al. [33] studied non-uniform step L1 scheme for the time-fractional MBE model with slope selection, and showed the L^2 norm error convergence of the scheme and energy stability. Zhang and Yang [24] established the maximum principle and energy stability of the linear CN scheme for the space-fractional AC equation. Zhang and Yang [25] proposed a first-order linear scheme with a stabilization term for the space-fractional AC equation and established the relevant theories of energy stability and the maximum principle.

The Scalar Auxiliary Variable (SAV) method was first proposed by Shen [11] to solve nonlinear partial differential equations, preserving the energy dissipation property. Many scholars have extended the SAV method to various phase field models; see, for example, [10, 20, 21, 22, 30, 17, 36]. There exist high-order schemes combined with the SAV method for gradient flow models. For instance, Huang et al. [8] developed the BDFk (k from one to five) schemes with the GSAV method for dissipative systems and analyzed the H^2 norm convergence of the AC and CH equations. Akrivis et al. [30] studied the linear RK schemes (up to fifth order) based on the SAV method for the AC and CH equations, proving the energy stability and convergence of the AC equation. Liu et al. [23] conducted the H^1 norm error analysis of the finite element method for the nonlinear subdiffusion equation. Gong et al. [28] proposed energy-stable high-order (up to sixth-order) numerical approaches using the Gaussian collocation method and the energy quadratization (EQ) method for gradient flow models. In [27], the authors proposed a fourth-order numerical scheme by combining the SAV method and the additive RK algorithm to solve gradient flow models and rigorously proved the convergence and energy stability of the proposed schemes. Based on the relaxed GSAV method, Zhang and Shen [9] investigated energy-stable implicit-explicit schemes (up to fifth-order) for dissipative systems and demonstrated that the modified energy more nearly approximates the original energy through numerical experiments.

In this work, the main purpose is to design an unconditionally energy-stable linear BDF6 scheme combined with the GSAV method for the SH equation. Although there exist some works on the SAV method for the SH equation, most of the existing

works primarily focus on energy stability. Due to the lack of convergence theory, we provide an H^2 norm convergence analysis for the proposed scheme. Zhou [13] studied the stability of the BDF6 scheme using energy methods for parabolic equations and derived the corresponding multipliers. This work validates the feasibility of the BDF6 scheme and supports error analysis. Furthermore, we implement the BDF6 scheme with the ESAV method, which also ensures energy stability. We discretize the spatial variable using the efficient Fourier spectral method and conduct numerical experiments to validate the stability and accuracy of the proposed scheme.

The remainder of this paper is structured as follows in Section 2, we propose the BDF6 scheme with GSAV method of the SH equation and prove that the scheme is unconditionally energy stable. We present the H^2 error analysis of our proposed scheme in Section 3. We present the BDF6 scheme with the ESAV method for the SH equation and analyze its energy stability in Section 4. Substantial experiments are executed to illustrate convergence and stability for the two schemes in Section 5.

2. The BDF6 scheme with GSAV method and energy stability

In this section, we introduce the GSAV method and devise the corresponding BDF6 scheme for the SH equation (1). We also review the Sobolev spaces $W^{k,p}$ with norm $\|\cdot\|_{W^{k,p}}$, where the space $H^k(\Omega)$ denotes $p=2$ where the corresponding norm is $\|\cdot\|_{H^k}$; $L^2(\Omega)$ denotes the space of $k=0, p=2$ with norm $\|\cdot\|$. Let $(\cdot,\cdot)$ represent the L^2-inner product. Let time step $\tau = T/N$ and $t_n = n\tau$, for $n \le N$, where N is a natural number.

We firstly introduce an important lemma about the regularity condition of the SH equation (see [16]) so that the exact solution is bounded.

Lemma 1. *Assume the initial solution $\phi_0 \in H^2(\Omega)$ and the following holds*

$$|f'(x)| < C(|x|^p + 1), \text{ for any } p > 0, \text{ if } d = 1, 2; \quad 0 < p < 4, \quad \text{if } d = 3,$$

$$|f''(x)| < C(|x|^{p'} + 1), \text{ for any } p' > 0, \text{ if } d = 1, 2; \quad 0 < p' < 3, \quad \text{if } d = 3,$$

where d denotes the space dimension. Then for any $T > 0$, the SH equation exists a unique solution $\phi \in C\left([0,T]; H^2(\Omega)\right) \cap L^2\left(0,T; H^4(\Omega)\right)$.

From the above Lemma 1, we conclude that there exists a positive constant C_Φ such that $\|\phi\|_{H^2} \le C_\Phi$ for any solution ϕ. For any $t \in (0,T]$, we denote the lower bound of the energy as follows:

$$\begin{aligned}
\mathcal{E}(\phi) &= \int_\Omega \left[\frac{1}{2}(\Delta\phi)^2 - |\nabla\phi|^2 + \frac{1}{4}\phi^4 - \frac{\beta}{3}\phi^3 + \frac{1-\epsilon}{2}\phi^2\right] \mathrm{d}x \\
&\ge \frac{1}{2}\|\Delta\phi\|_{L^2}^2 - \|\nabla\phi\|_{L^2}^2 + \frac{1}{4}\|\phi\|_{L^4}^4 - \frac{\beta}{3}\|\phi\|_{L^3}^3 + \frac{1-\epsilon}{2}\|\phi\|_{L^2}^2 \\
&\ge \frac{1}{2}\|\Delta\phi\|_{L^2}^2 + \frac{1-\epsilon}{2}\|\phi\|_{L^2}^2 + \left(\frac{1}{4} - \frac{\varepsilon\beta}{3}\right)\|\phi\|_{L^4}^4 - \|\nabla\phi\|_{L^2}^2 - \frac{\beta}{12\varepsilon}\|\phi\|_{L^2}^2 \\
&\ge \frac{1}{2}\|\Delta\phi\|_{L^2}^2 + \frac{1-\epsilon}{2}\|\phi\|_{L^2}^2 - \max\left\{1, \frac{\beta^2}{9}\right\}\|\phi\|_{H^1}^2 \\
&\ge -\max\left\{1, \frac{\beta^2}{9}, \frac{1-\epsilon}{2}\right\}\|\phi\|_{H^2}^2,
\end{aligned}$$

where we use the inequality $\int_\Omega \phi^3 \mathrm{d}x \le \|\phi\|_{L^4}^2 \|\phi\|_{L^2}$ and set $\varepsilon = \frac{3\beta}{4}$. On this basis, we construct the auxiliary variable $R(t) = E(\phi)(t) := \mathcal{E}(\phi) + C_0 > 0$, $C_0 > 0$. Then

the problem (1) can be rewritten as below

$$\phi_t = -\left(\Delta^2\phi + 2\Delta\phi + f(\phi)\right),$$
$$\frac{dE}{dt} = -\frac{R}{E(\phi)}\left(\frac{\delta E(\phi)}{\delta\phi}, \frac{\delta E(\phi)}{\delta\phi}\right).$$

Now we present the BDF6 scheme with GSAV method for the problem (1) as

$$\frac{\alpha_6\overline{\phi}^{n+1} - A_6(\phi^n)}{\tau} = -(\Delta^2 + 2\Delta)\overline{\phi}^{n+1} - f(B_6(\overline{\phi}^n)), \tag{4a}$$

$$\frac{R^{n+1} - R^n}{\tau} = -\frac{R^{n+1}}{E(\overline{\phi}^{n+1})}\left(\frac{\delta E(\overline{\phi}^{n+1})}{\delta\phi}, \frac{\delta E(\overline{\phi}^{n+1})}{\delta\phi}\right), \tag{4b}$$

$$\xi^{n+1} = \frac{R^{n+1}}{E(\overline{\phi}^{n+1})}, \tag{4c}$$

$$\phi^{n+1} = \eta^{n+1}\overline{\phi}^{n+1}, \text{ with } \eta^{n+1} = 1 - (1-\xi^{n+1})^7, \tag{4d}$$

where

$$\alpha_6 = \frac{49}{20},\ A_6(\phi^n) = 6\phi^n - \frac{15}{2}\phi^{n-1} + \frac{20}{3}\phi^{n-2} - \frac{15}{4}\phi^{n-3} + \frac{6}{5}\phi^{n-4} - \frac{1}{6}\phi^{n-5};$$
$$B_6(\overline{\phi}^n) = 6\overline{\phi}^n - 15\overline{\phi}^{n-1} + 20\overline{\phi}^{n-2} - 15\overline{\phi}^{n-3} + 6\overline{\phi}^{n-4} - \overline{\phi}^{n-5}.$$

Remark 1: To avoid affecting the overall convergence order of the BDF6 scheme, we adopt the sixth-order implicit RK method to solve the numerical solutions for the first 5 time steps.

Theorem 1. *The scheme (4) satisfies energy dissipation law as follows*

$$R^{n+1} - R^n = -\tau\xi^{n+1}\left(\frac{\delta E(\overline{\phi}^{n+1})}{\delta\phi}, \frac{\delta E(\overline{\phi}^{n+1})}{\delta\phi}\right) \le 0. \tag{5}$$

Moreover, assume $E(\phi) = \frac{1}{2}(\Delta^2\phi, \phi) + E_1(\phi)$ and $E_1(\phi)$ has a lower bound, there exists a positive constant C_ϕ makes

$$\left(\Delta^2\phi^{n+1}, \phi^{n+1}\right) \le C_\phi^2. \tag{6}$$

Proof. As mentioned in the definition $R = E(\phi) > 0$, we can infer $R^n > 0$, $E(\overline{\phi}^{n+1}) > 0$, and we can obtain

$$R^{n+1} = \frac{R^n}{1 + \tau\left(\frac{\delta E(\overline{\phi}^{n+1})}{\delta\phi}, \frac{\delta E(\overline{\phi}^{n+1})}{\delta\phi}\right)/E(\overline{\phi}^{n+1})} \ge 0,$$

and $\xi^{n+1} \ge 0$ from scheme (4c). Thus, the inequality (5) holds.

Denote $R^0 = E(\phi(\cdot, 0))$, the formula (5) implies $R^n \le R^0$. Without loss of generality, we suppose $E_1(\phi) > 1$, then from (4c) yields

$$|\xi^{n+1}| = \frac{R^{n+1}}{E(\overline{\phi}^{n+1})} \le \frac{2R^0}{\left(\Delta^2\overline{\phi}^{n+1}, \overline{\phi}^{n+1}\right) + 2}. \tag{7}$$

So we can observe that ξ^{n+1} is bounded. According to the formula (4d), we get $|\eta^{n+1}| = |\xi^{n+1}P_6(\xi^{n+1})|$, where $P_6(x)$ denotes a polynomial of degree less than 6. Therefore, we can deduce that there exists positive constant $C_\phi > 0$ such that

$$|\eta^{n+1}| \le \frac{C_\phi}{\left(\Delta^2\overline{\phi}^{n+1}, \overline{\phi}^{n+1}\right) + 2},$$

and

$$\left(\Delta^2\phi^{n+1},\phi^{n+1}\right)=(\eta^{n+1})^2\left(\Delta^2\overline{\phi}^{n+1},\overline{\phi}^{n+1}\right)\le C_\phi^2.$$

The proof is completed. □

3. H^2 norm error estimate of the scheme (4)

In the section, we present the rigorous convergence analysis for the scheme (4). We review stability of the BDF6 scheme (see [29]).

Lemma 2. *The set of numbers* $\kappa_0=-\frac{31}{32},\kappa_1=\frac{13}{9},\kappa_2=-\frac{25}{36},\kappa_3=\frac{1}{9},\kappa_4=\kappa_5=\kappa_6=0$ *is a multiplier of the* $BDF6$ *scheme, then there exists a positive definite symmetric matrix* $G=\{g_{ij}\}\in\mathbb{R}^{6,6}$ *and real* $\theta_0,\cdots,\theta_6$ *such that*

$$\begin{aligned}&\left(\alpha_6\phi^{n+1}-A_6(\phi^n),\phi^{n+1}-\sum_{j=1}^{3}\kappa_j\phi^{n+1-j}\right)\\&=\sum_{i,j=1}^{6}g_{ij}(\phi^{n+1+i-6},\phi^{n+1+j-6})-\sum_{i,j=1}^{6}g_{ij}(\phi^{n+i-6},\phi^{n+j-6})\\&\quad+\left\|\sum_{i=0}^{6}\theta_i\phi^{n+1+i-6}\right\|^2,\end{aligned}\tag{8}$$

with $6\le n+1\le N$. *Furthermore, the following inequality holds*

$$\sum_{n=5}^{m}\left(\phi^{n+1},\phi^{n+1}-\sum_{j=1}^{3}\kappa_j\phi^{n+1-j}\right)\ge\frac{1}{32}\sum_{n=3}^{m}\|\phi^{n+1}\|^2.\tag{9}$$

Theorem 2. *Given initial condition* $\overline{\phi}^0=\phi^0=\phi_0(x)$ *and* $R^0=E(\phi^0)$, *we assume Lemma 1 holds and the exact function satisfies the following conditions*

$$\phi\in C([0,T],H^3(\Omega)),\frac{\partial^j\phi}{\partial t^j}\in L^2\left(0,T;H^2(\Omega)\right),\ 1\le j\le 6,\ \frac{\partial^7\phi}{\partial t^7}\in L^2\left(0,T;H^1(\Omega)\right).$$

Let $\overline{\phi}^n$ *and* ϕ^n *be computed by scheme (4). Then, when* $\tau\le\min\left\{\frac{1}{1+2C_\xi^7},\frac{\lambda_G}{2C},\frac{1}{2}\right\}$, *it holds*

$$\|\overline{\phi}^n-\phi(\cdot,t_n)\|_{H^2},\ \|\phi^n-\phi(\cdot,t_n)\|_{H^2}\le C\tau^6,\quad n\le N,\tag{10}$$

where positive constants C_ξ *and* C *are related to* T, Ω.

Proof. We can get the numerical solutions of the first 5 time steps $\overline{\phi}^k=\phi^k$ $(k=1,\cdots,5)$ by the sixth-order implicit RK method, which meets $\|\phi^k-\phi(t_k)\|_{H^2}=O(\tau^6)$ and $\|\Delta^2\phi^k\|\le C$. The corresponding $R^k=E(\phi^k)$ can also be calculated.

The main purpose is to prove

$$|1-\xi^n|\le C_\xi\tau,\ \forall\ n\le N,\tag{11}$$

it is clear that inequality (11) holds for $\phi^k=\overline{\phi}^k$ $(k=1,\cdots,5)$. Next, we adopt the mathematical induction and suppose $|1-\xi^n|\le C_\xi\tau$ holds for $n\le m$, then we set two parts to prove formula (11) holds for $n=m+1\le N$. According to assumed condition $|1-\xi^n|\le C_\xi\tau$, $n\le m$, we can get from formula (4d)

$$1-\frac{\tau^6}{2}\le|\eta^n|\le 1+\frac{\tau^6}{2},\ n\le m,$$

when time step $\tau \leq \min\left\{\frac{1}{2C_\xi^7}, 1\right\}$. Combined with the inequality (6) yields

$$\|\phi^n\|_{H^2} \leq C_\phi,\ \|\overline{\phi}^n\|_{H^2} \leq 2C_\phi, \forall\ n \leq m. \tag{12}$$

Step 1: Estimates for $\|\overline{e}^{n+1}\|_{H^2}$ and $\|\overline{e}^{n+1}\|_{H^4}$ for $0 \leq n \leq m$. According to the regularity result of Lemma 1, there exists a sufficiently large positive constant C_Φ such that

$$\|\phi(t)\|_{H^2} \leq C_\Phi,\quad t \leq T. \tag{13}$$

By the Sobolev embedding theorem $H^2(\Omega) \subset L^\infty(\Omega)$, we have

$$\|f^{(i)}(\phi(t))\|_{L^\infty} \leq C_\Phi,\quad t \leq T,\quad \|f^{(i)}(\overline{\phi}^n)\|_{L^\infty} \leq C_\phi, \forall\ n \leq m,\quad i = 0, 1, 2, 3. \tag{14}$$

From scheme (4a), we can get error equation as

$$\alpha_6\overline{e}^{n+1} - A_6(\overline{e}^n) = A_6(\overline{\phi}^n) - A_6(\phi^n) - \tau(\Delta^2 + 2\Delta)\overline{e}^{n+1} + Y^n + \tau U^n, \tag{15}$$

where $\overline{e}^n = \phi(t_n) - \overline{\phi}^n$, Y^n denotes as

$$\begin{aligned} Y^n =& \alpha_6(\phi(t_{n+1})) - A_6(\phi(t_n)) - \tau\phi_t(t_{n+1}) \\ =& \sum_{i=1}^{6} a_i \int_{t_{n+1-i}}^{t_{n+1}} (t_{n+1-i} - s)^6 \frac{\partial^7 \phi}{\partial t^7}(s)\mathrm{d}s, \end{aligned} \tag{16}$$

with a_i are relevant to the coefficients of A_6. U^n is given by

$$U^n = f(B_6(\overline{\phi}^n)) - f(\phi(t_{n+1})).$$

Taking the inner product of (15) with $\overline{v}^{n+1} := \overline{e}^{n+1} - \frac{13}{9}\overline{e}^n + \frac{25}{36}\overline{e}^{n-1} - \frac{1}{9}\overline{e}^{n-2}$, and using Lemma 2, we have

$$\begin{aligned} &\sum_{i,j=1}^{6} g_{ij}(\overline{e}^{n+1+i-6}, \overline{e}^{n+1+j-6}) - \sum_{i,j=1}^{6} g_{i,j}(\overline{e}^{n+i-6}, \overline{e}^{n+j-6}) + \left\|\sum_{i=1}^{6} \theta_i \overline{e}^{n+1+i-6}\right\|^2 \\ &= \left(A_6(\overline{\phi}^n) - A_6(\phi^n), \overline{v}^{n+1}\right) - \tau\left((\Delta^2 + 2\Delta)\overline{e}^{n+1}, \overline{v}^{n+1}\right) \\ &\quad + \left(Y^n, \overline{v}^{n+1}\right) + \tau\left(U^n, \overline{v}^{n+1}\right). \end{aligned} \tag{17}$$

Next, we analyze the estimates on right hand side of formula (17). Note that $|\eta^n - 1| \leq |1 - \xi^n|^7 \leq C_\xi^7\tau^7$, $\forall\ n \leq m$, we have

$$\begin{aligned} \left|\left(A_6(\overline{\phi}^n) - A_6(\phi^n), \overline{v}^{n+1}\right)\right| &\leq \frac{\|A_6(\overline{\phi}^n) - A_6(\phi^n)\|^2}{2\tau} + \tau\sum_{i=0}^{3}\|\overline{e}^{n+1-i}\|^2 \\ &\leq CC_\xi^{14}\tau^{13} + \tau\sum_{i=0}^{3}\|\overline{e}^{n+1-i}\|^2. \end{aligned} \tag{18}$$

Applying the Cauchy-Schwarz inequality, we obtain

$$\tau\left|\left((\Delta^2 + 2\Delta)\overline{e}^{n+1}, \overline{v}^{n+1}\right)\right| \leq \tau\sum_{i=0}^{3}\|\Delta\overline{e}^{n+1-i}\|^2 + 2\tau\sum_{i=0}^{3}\|\nabla\overline{e}^{n+1-i}\|^2. \tag{19}$$

For term Y^n, it follows from the Schwarz inequality

$$\|Y^n\|^2 \leq C\tau^{12}\int_\Omega\left(\int_{t_{n-5}}^{t_{n+1}} 1 \cdot \frac{\partial^7\phi}{\partial t^7}(s)\mathrm{d}s\right)^2 \mathrm{d}x \leq C\tau^{13}\int_{t_{n-5}}^{t_{n+1}}\left\|\frac{\partial^7\phi}{\partial t^7}(s)\right\|^2 \mathrm{d}s.$$

So we get the estimate

$$\begin{aligned}\left|\left(Y^n,\overline{v}^{n+1}\right)\right| &\le \frac{1}{2\tau}\|Y^n\|^2+2\tau\sum_{i=0}^{3}\|\overline{e}^{n+1-i}\|^2\\ &\le C\tau^{12}\int_{t_{n-5}}^{t_{n+1}}\left\|\frac{\partial^7\phi}{\partial t^7}(s)\right\|^2\mathrm{d}s+2\tau\sum_{i=0}^{3}\|\overline{e}^{n+1-i}\|^2.\end{aligned}\tag{20}$$

Noticing that $\phi^n,\phi(t)$ are bounded and citing formula (14), we have

$$\begin{aligned}|U^n| &= \left|f(B_6(\overline{\phi}^n))-f(B_6(\phi(t_n)))+f(B_6(\phi(t_n)))-f(\phi(t_{n+1}))\right|\\ &\le C|B_6(\overline{e}^n)|+C|B_6(\phi(t_n))-\phi(t_{n+1})|\\ &\le C|B_6(\overline{e}^n)|+C\left|\sum_{i=1}^{6}b_i\int_{t_{n+1-i}}^{t_{n+1}}(t_{n+1-i}-s)^5\frac{\partial^6\phi}{\partial t^6}(s)\mathrm{d}s\right|,\end{aligned}$$

where $b_1=-\frac{6}{5!}$, $b_2=\frac{15}{5!}$, $b_3=-\frac{20}{5!}$, $b_4=\frac{15}{5!}$, $b_5=-\frac{6}{5!}$ and $b_6=\frac{1}{5!}$ can be determined by Taylor's formula. Combining the Cauchy-Schwarz inequality, we can obtain

$$\begin{aligned}\tau\left|\left(U^n,\overline{v}^{n+1}\right)\right| &\le C\tau\|B_6(\overline{e}^n)\|^2+2\tau\sum_{i=0}^{3}\|\overline{e}^{n+1-i}\|^2+C\tau^{12}\int_{t_{n-5}}^{t_{n+1}}\left\|\frac{\partial^6\phi}{\partial t^6}(s)\right\|^2\mathrm{d}s\\ &\le C\tau\sum_{i=0}^{6}\|\overline{e}^{n+1-i}\|^2+C\tau^{12}\int_{t_{n-5}}^{t_{n+1}}\left\|\frac{\partial^6\phi}{\partial t^6}(s)\right\|^2\mathrm{d}s.\end{aligned}\tag{21}$$

In the light of the inequalities (18), (19), (20) and (21), we arrive at

$$\begin{aligned}&\sum_{i,j=1}^{6}g_{i,j}(\overline{e}^{n+1+i-6},\overline{e}^{n+1+j-6})-\sum_{i,j=1}^{6}g_{i,j}(\overline{e}^{n+i-6},\overline{e}^{n+j-6})+\left\|\sum_{i=1}^{6}\theta_i\overline{e}^{n+1+i-6}\right\|^2\\ &\le C\tau\sum_{i=0}^{6}\|\overline{e}^{n+1-i}\|_{H^2}^2+C\tau^{12}\left(\int_{t_{n-5}}^{t_{n+1}}\left\|\frac{\partial^7\phi}{\partial t^7}(s)\right\|+\int_{t_{n-5}}^{t_{n+1}}\left\|\frac{\partial^6\phi}{\partial t^6}(s)\right\|^2+C_\xi^{14}\right)\mathrm{d}s.\end{aligned}\tag{22}$$

Taking the sum for n from 5 to m for formula (22), we can get

$$\lambda_G\|\overline{e}^{m+1}\|^2\le C\tau\sum_{n=0}^{m+1}\|\overline{e}^n\|_{H^2}^2+C\tau^{12}\int_0^T\left(\left\|\frac{\partial^7\phi}{\partial t^7}(s)\right\|+\left\|\frac{\partial^6\phi}{\partial^6}(s)\right\|^2+C_\xi^{14}\right)\mathrm{d}s,\tag{23}$$

where the matrix G is positive definite and the smallest eigenvalue $\lambda_G>0$.

Implementing the same procedure, we can get the estimates of $\|\nabla\overline{e}^{m+1}\|$ and $\|\Delta\overline{e}^{m+1}\|$. Making the inner product on the both sides of (15) with

$-3\Delta\overline{v}^{n+1} := -3\left(\Delta\overline{e}^{n+1} - \frac{13}{9}\Delta\overline{e}^{n} + \frac{25}{36}\Delta\overline{e}^{n-2} - \frac{1}{9}\Delta\overline{e}^{n-3}\right)$, we have

$$\begin{aligned}
&3\sum_{i,j=1}^{6} g_{i,j}(\nabla\overline{e}^{n+1+i-6}, \nabla\overline{e}^{n+1+j-6}) - 3\sum_{i,j=1}^{6} g_{i,j}(\nabla\overline{e}^{n+i-6}, \nabla\overline{e}^{n+j-6}) \\
&+ 3\left\|\sum_{i=1}^{6}\theta_i\nabla\overline{e}^{n+1+i-6}\right\|^2 - 3\tau\left(\Delta^2\overline{e}^{n+1}, \Delta\overline{v}^{n+1}\right) \\
=& -3\left(A_6(\overline{\phi}^n) - A_6(\phi^n), \Delta\overline{v}^{n+1}\right) - 3\left(Y^n, \Delta\overline{v}^{n+1}\right) - 3\tau\left(U^n, \Delta\overline{v}^{n+1}\right) \\
&+ 6\tau\left(\Delta\overline{e}^{n+1}, \Delta\overline{v}^{n+1}\right). \qquad (24)
\end{aligned}$$

The estimates of the right-hand terms in formula (24) coincide with those in inequalities (18), (20) and (21), then taking the sum for n from 5 to m and combining the formula (9), we can obtain

$$\begin{aligned}
&\lambda_G\|\nabla\overline{e}^{m+1}\|^2 + 3\tau\sum_{n=5}^{m}\left(\nabla\Delta\overline{e}^{n+1}, \nabla\Delta\overline{v}^{n+1}\right) \\
\le& C\tau^{12}\int_0^T\left(\left\|\frac{\partial^7\phi}{\partial t^7}(s)\right\|^2 + \left\|\frac{\partial^6\phi}{\partial t^6}(s)\right\|^2 + C_\xi^{14}\right)\mathrm{d}s + C\tau\sum_{n=0}^{m+1}\|\overline{e}^n\|_{H^2}^2. \qquad (25)
\end{aligned}$$

Taking the inner product of (15) with $\Delta^2\overline{v}^{n+1} := \Delta^2\overline{e}^{n+1} - \frac{13}{9}\Delta^2\overline{e}^{n} + \frac{25}{36}\Delta^2\overline{e}^{n-1} - \frac{1}{9}\Delta^2\overline{e}^{n-2}$, one can get

$$\begin{aligned}
&\sum_{i,j=1}^{6} g_{i,j}(\Delta\overline{e}^{n+1+i-6}, \Delta\overline{e}^{n+1+j-6}) - \sum_{i,j=1}^{6} g_{i,j}(\Delta\overline{e}^{n+i-6}, \Delta\overline{e}^{n+j-6}) \\
&+ \left\|\sum_{i=1}^{6}\theta_i\Delta\overline{e}^{n+1+i-6}\right\|^2 + \tau\left(\Delta^2\overline{e}^{n+1}, \Delta^2\overline{v}^{n+1}\right) \\
=& \left(A_6(\overline{\phi}^n) - A_6(\phi^n), \Delta^2\overline{v}^{n+1}\right) + \left(Y^n, \Delta^2\overline{v}^{n+1}\right) + \tau\left(U^n, \Delta^2\overline{v}^{n+1}\right) \\
&+ 2\tau\left(\nabla\Delta\overline{e}^{n+1}, \nabla\Delta\overline{v}^{n+1}\right). \qquad (26)
\end{aligned}$$

Next, we estimate the right-hand side of formula (26). By using the formula (18), we get

$$\left|\left(A_6(\overline{\phi}^n) - A_6(\phi^n), \Delta^2\overline{v}^{n+1}\right)\right| \le CC_\xi^{14}\tau^{13} + \frac{\tau}{384}\sum_{i=0}^{3}\|\nabla\Delta\overline{e}^{n+1-i}\|^2. \qquad (27)$$

According to the Cauchy-Schwarz inequality for terms Y^n and U^n, we have the estimate

$$\begin{aligned}
\left|\left(Y^n, \Delta^2\overline{v}^{n+1}\right)\right| &\le \frac{C}{\tau}\|\nabla Y^n\|^2 + \frac{\tau}{384}\sum_{i=0}^{3}\|\nabla\Delta\overline{e}^{n+1-i}\|^2 \\
&\le C\tau^{12}\int_{t_{n-5}}^{t_{n+1}}\left\|\frac{\partial^7\phi}{\partial t^7}(s)\right\|_{H^1}^2\mathrm{d}s + \frac{\tau}{384}\sum_{i=0}^{3}\|\nabla\Delta\overline{e}^{n+1-i}\|^2, \qquad (28)
\end{aligned}$$

and

$$\begin{aligned}\tau\left|\left(U^n,\Delta^2\overline{v}^{n+1}\right)\right|\leq&C\tau\|\nabla U^n\|^2+\frac{\tau}{384}\sum_{i=0}^{3}\|\nabla\Delta\overline{e}^{n+1-i}\|^2\\ \leq&C\tau\|B_6(\overline{e}^n)\|_{H^1}^2+C\tau^{12}\int_{t_{n-5}}^{t_{n+1}}\left\|\frac{\partial^6\phi}{\partial t^6}(s)\right\|_{H^1}^2\mathrm{d}s\\ &+\frac{\tau}{384}\sum_{i=0}^{3}\|\nabla\Delta\overline{e}^{n+1-i}\|^2.\end{aligned}\tag{29}$$

Using the inequalities (27), (28) and (29), and summing n from 5 to m for formula (26) yields

$$\begin{aligned}&\lambda_G\|\Delta\overline{e}^{m+1}\|^2+\tau\sum_{n=5}^{m}\left(\Delta^2\overline{e}^{n+1},\Delta^2\overline{v}^{n+1}\right)\\ \leq&C\tau^{12}\int_0^T\left(\left\|\frac{\partial^7\phi}{\partial t^7}(s)\right\|_{H^1}^2+\left\|\frac{\partial^6\phi}{\partial t^6}(s)\right\|_{H^1}^2+C_\xi^{14}\right)\mathrm{d}s+C\tau\sum_{n=0}^{m+1}\|\overline{e}^n\|_{H^2}^2\\ &+\frac{\tau}{32}\sum_{n=3}^{m+1}\|\nabla\Delta\overline{e}^n\|^2+2\tau\sum_{n=5}^{m}\left(\nabla\Delta\overline{e}^{n+1},\nabla\Delta\overline{v}^{n+1}\right).\end{aligned}\tag{30}$$

Adding the formulas (23), (25) and (30), and combining the formula (9), we derive

$$\begin{aligned}&\lambda_G\|\overline{e}^{m+1}\|_{H^2}^2+\frac{\tau}{32}\sum_{n=3}^{m+1}\|\Delta^2\overline{e}^n\|^2\\ \leq&C\tau^{12}\int_0^T\left(\left\|\frac{\partial^7\phi}{\partial t^7}(s)\right\|_{H^1}^2+\left\|\frac{\partial^6\phi}{\partial t^6}(s)\right\|_{H^1}^2+C_\xi^{14}\right)\mathrm{d}s\\ &+C\tau\sum_{n=0}^{m+1}\|\overline{e}^n\|_{H^2}^2.\end{aligned}\tag{31}$$

By referencing the discrete Grönwall inequality, we have

$$\begin{aligned}&\|\overline{e}^{m+1}\|_{H^2}^2+\frac{1}{\lambda_G}\frac{\tau}{32}\sum_{n=3}^{m+1}\|\Delta^2\overline{e}^n\|^2\\ \leq&\frac{2}{\lambda_G}C\exp((1-\tau)^{-1}T)\tau^{12}\int_0^T\left(\left\|\frac{\partial^7\phi}{\partial t^7}(s)\right\|_{H^1}^2+\left\|\frac{\partial^6\phi}{\partial t^6}(s)\right\|_{H^1}^2+C_\xi^{14}\right)\mathrm{d}s\\ :=&C_2\left(1+C_\xi^{14}\right)\tau^{12},\end{aligned}\tag{32}$$

when time step $\tau\leq\min\{\frac{\lambda_G}{2C},\frac{1}{2}\}$, C_2 is independent of τ and denotes as

$$C_2:=\frac{2}{\lambda_G}C\exp(2T)\max\left\{\int_0^T\left(\left\|\frac{\partial^7\phi}{\partial t^7}(s)\right\|_{H^1}^2+\left\|\frac{\partial^6\phi}{\partial t^6}(s)\right\|_{H^1}^2\right)\mathrm{d}s,2,T\right\}.$$

In particular, the relation (32) implies

$$\|\overline{e}^{m+1}\|_{H^2}\leq\sqrt{C_2(1+C_\xi^{14})}\tau^6,\tag{33}$$

$$\left(\tau\sum_{n=5}^{m+1}\|\Delta^2\overline{e}^n\|^2\right)^{\frac{1}{2}}\leq\sqrt{32\lambda_GC_2(1+C_\xi^{14})}\tau^6,\ \forall\ 1\leq m+1\leq N.\tag{34}$$

Combined with condition $\|\phi(t)\|_{H^2} \leq C_\Phi$, we further derive

$$\|\overline{\phi}^{m+1}\|_{H^2} \leq \sqrt{C_2(1+C_\xi^{14})}\tau^6 + C_\Phi.$$

Note that $H^2(\Omega) \subset L^\infty(\Omega)$, we can get the terms $\|f(\overline{\phi}^{m+1})\|_{L^\infty}$ and $\|f'(\overline{\phi}^{m+1})\|_{L^\infty}$ are bounded.

Step 2: Estimate $|1-\xi^{m+1}|$. By direct calculation, it is clear that

(35)
$$R_{tt} = \int_\Omega \left(|\Delta\phi_t|^2 + \Delta\phi\Delta\phi_{tt} - 2|\nabla\phi_t|^2 - 2\nabla\phi\cdot\nabla\phi_{tt} + f'(\phi)\phi_t^2 + f(\phi)\phi_{tt}\right)\mathrm{d}x.$$

From (4b), the error equation is

$$w^{n+1} - w^n = \tau\left(\|F(\phi(t_{n+1}))\|^2 - \frac{R^{n+1}}{E(\overline{\phi}^{n+1})}\|F(\overline{\phi}^{n+1})\|^2\right) + Q^{n+1}, \tag{36}$$

where $w^n = R^n - R(t_n)$, $V(\phi) = \frac{\delta E}{\delta\phi} = (\Delta^2 + 2\Delta)\phi + f(\phi)$ and

$$Q^{n+1} = R(t_n) - R(t_{n+1}) + \tau R_t(t_{n+1}) = \int_{t_n}^{t_{n+1}} (s-t_n)R_{tt}\mathrm{d}s.$$

Summing equation (36) over n from 0 to m with $w^0 = 0$, we have

$$w^{m+1} = \tau\sum_{n=0}^{m}\left(\|V(\phi(t_{n+1}))\|^2 - \frac{R^{n+1}}{E(\overline{\phi}^{n+1})}\|V(\overline{\phi}^{n+1})\|^2\right) + \sum_{n=0}^{m} Q^{n+1}. \tag{37}$$

The first term of the right-hand side of the formula (37) has

$$\begin{aligned}
&\left|\|V(\phi(t_{n+1}))\|^2 - \frac{R^{n+1}}{E(\overline{\phi}^{n+1})}\|V(\overline{\phi}^{n+1})\|^2\right| \\
\leq&\|V(\phi(t_{n+1}))\|^2\left|1 - \frac{R^{n+1}}{E(\overline{\phi}^{n+1})}\right| + \frac{R^{n+1}}{E(\overline{\phi}^{n+1})}\left|\|V(\phi(t_{n+1}))\|^2 - \|V(\overline{\phi}^{n+1})\|^2\right| \\
:=&Z_1 + Z_2. \qquad (38)
\end{aligned}$$

For Z_1, due to $\phi(t)$ and R^{n+1} are bounded, it follows

$$\begin{aligned}
Z_1 \leq& C\left|1 - \frac{R^{n+1}}{E(\overline{\phi}^{n+1})}\right| \\
\leq& C\left|\frac{R(t_{n+1})}{E(\phi(t_{n+1}))} - \frac{R^{n+1}}{E(\phi(t_{n+1}))}\right| + C\left|\frac{R^{n+1}}{E(\phi(t_{n+1}))} - \frac{R^{n+1}}{E(\overline{\phi}^{n+1})}\right| \\
\leq& C\left(|w^{n+1}| + |E(\phi(t_{n+1})) - E(\overline{\phi}^{n+1})|\right). \qquad (39)
\end{aligned}$$

According to the bounded conditions (12) and (13), we can get

$$\begin{aligned}
\left|E(\phi(t_{n+1})) - E(\overline{\phi}^{n+1})\right| \leq& \frac{1}{2}\left(\|\Delta\phi(t_{n+1})\| + \|\Delta\overline{\phi}^{n+1}\|\right)\left\|\Delta\phi(t_{n+1}) - \Delta\overline{\phi}^{n+1}\right\| \\
&+ \left(\|\nabla\phi(t_{n+1})\| + \|\nabla\overline{\phi}^{n+1}\|\right)\left\|\nabla\phi(t_{n+1}) - \nabla\overline{\phi}^{n+1}\right\| \\
&+ \int_\Omega\left|F\left(\phi(t_{n+1})\right) - F(\overline{\phi}^{n+1})\right|\mathrm{d}x \\
\leq& C\left(\|\Delta\overline{e}^{n+1}\| + \|\nabla\overline{e}^{n+1}\| + \|\overline{e}^{n+1}\|\right). \qquad (40)
\end{aligned}$$

Thereby, we have $Z_1 \leq C\|\overline{e}^{n+1}\|_{H^2} + |w^{n+1}|$. For Z_2, we can obtain

$$\begin{aligned} Z_2 &\leq C\left|\|V(\phi(t_{n+1}))\|^2 - \|V(\overline{\phi}^{n+1})\|^2\right| \\ &\leq C\left\|V(\phi(t_{n+1})) - V(\overline{\phi}^{n+1})\right\|\left(\|V(\phi(t_{n+1}))\| + \|V(\overline{\phi}^{n+1})\|\right) \\ &\leq C\left(\|\Delta^2\overline{e}^{n+1}\| + \|\Delta\overline{e}^{n+1}\| + \left\|f(\phi(t_{n+1})) - f(\overline{\phi}^{n+1})\right\|\right) \\ &\leq C\left(\|\Delta^2\overline{e}^{n+1}\| + \|\Delta\overline{e}^{n+1}\| + \|\overline{e}^{n+1}\|\right). \end{aligned} \tag{41}$$

From the formula (35), we get the estimate of Q^{n+1} as

$$|Q^{n+1}| \leq C\tau\int_{t_n}^{t_{n+1}} |R_{tt}(s)|\mathrm{d}s \leq C\tau\int_{t_n}^{t_{n+1}} \left(\|\phi_t(s)\|_{H^2}^2 + \|\phi_{tt}(s)\|_{H^2}\right)\mathrm{d}s. \tag{42}$$

Thus, it follows from the formulas (39), (40), (41), (42), (33) and (34) that

$$\begin{aligned} |w^{m+1}| \leq& \tau\sum_{n=0}^{m}\left|\|V(\phi(t_{n+1}))\|^2 - \frac{R^{n+1}}{E(\overline{\phi}^{n+1})}\|V(\overline{\phi}^{n+1})\|\right| + \sum_{n=0}^{m}|Q^{n+1}| \\ \leq& C\tau\sum_{n=0}^{m}|w^{n+1}| + C\tau\sum_{n=0}^{m}\|\overline{e}^{n+1}\|_{H^2} + C\tau\sum_{n=0}^{m}\|\Delta^2\overline{e}^{n+1}\| \\ &+ C\tau\int_0^T \left(\|\phi_t(s)\|_{H^2}^2 + \|\phi_{tt}(s)\|_{H^2}\right)\mathrm{d}s \\ \leq& C\tau\sum_{n=0}^{m}|w^{n+1}| + C\sqrt{32\lambda_G C_2(1+C_\xi^{14})}\tau^6 + C\tau, \end{aligned} \tag{43}$$

where it follows from the Hölder inequality, the formula (34) and the assumed condition $\|\Delta^2\overline{e}^k\| \leq C, k = 1, \cdots, 5$, we have

$$\left(\tau\sum_{n=1}^{m+1}\|\Delta^2\overline{e}^n\|\right) \leq \left(\tau\sum_{n=1}^{m+1}\|\Delta^2\overline{e}^n\|^2\right)^{\frac{1}{2}}\left(\tau\sum_{n=1}^{m+1}1\right)^{\frac{1}{2}} \leq C\sqrt{32\lambda_G C_2(1+C_\xi^{14})}\tau^6.$$

By referencing the discrete Grönwall inequality with $\tau \leq \frac{1}{C}$ yields $|w^{m+1}| \leq C\tau$. Furthermore, using the formulas (4c), (39) and (40), we obtain

$$\begin{aligned} |1-\xi^{m+1}| \leq& C\left(\left|E(\phi(t_{m+1})) - E(\overline{\phi}^{m+1})\right| + |w^{m+1}|\right) \\ \leq& C(\|\overline{e}^{m+1}\|_{H^2} + |w^{m+1}|) \leq C\tau. \end{aligned} \tag{44}$$

In the view of formula (4d), we get

$$\begin{aligned} &|\eta^{m+1} - 1| \leq |1-\xi^{m+1}|^7 \leq C\tau^7, \\ &\|\phi^{m+1} - \overline{\phi}^{m+1}\|_{H^2} \leq |\eta^{m+1}-1|\|\overline{\phi}^{m+1}\|_{H^2} \leq 2C_\phi C|\eta^{m+1}-1|, \end{aligned}$$

and easily infer that

$$\|e^{m+1}\|_{H^2}^2 \leq \|\overline{e}^{m+1}\|_{H^2}^2 + \|\phi^{m+1} - \overline{\phi}^{m+1}\|_{H^2}^2 \leq C_2\left(1+C_\xi^{14}\right)\tau^{12} + C\tau^{14}.$$

The proof ends here. □

4. ESAV method

In this section, we present the BDF6 scheme combined with the ESAV method for the SH equation.

Defining auxiliary variable $R(t) := \exp(\mathcal{E}(\phi(t)))$, and we can reformulate the problem (1) as

$$\phi_t = -(\Delta^2 + 2\Delta)\phi - f(\phi),$$
$$\frac{dR}{dt} = -R\left(\frac{\delta \mathcal{E}}{\delta \phi}, \frac{\delta \mathcal{E}}{\delta \phi}\right).$$

Analogously, the BDF6 scheme with the ESAV method as follows

$$\frac{\alpha_6 \phi^{n+1} - A_6(\phi^n)}{\tau} = -(\Delta^2 + 2\Delta)\phi^{n+1} - \eta^{n+1} f(B_6(\phi^n)), \tag{45a}$$

$$\frac{R^{n+1} - R^n}{\tau} = -R^{n+1}\left(\frac{\delta \mathcal{E}(B_6(\phi^n))}{\delta \phi}, \frac{\delta \mathcal{E}(B_6(\phi^n))}{\delta \phi}\right), \tag{45b}$$

$$\xi^{n+1} = \frac{R^{n+1}}{\exp(\mathcal{E}(B_6(\phi^n)))}, \quad \eta^{n+1} = 1 - (1 - \xi^{n+1})^7. \tag{45c}$$

Remark 2. It is noted that the exponential function is a rapidly growing function, which can lead to the numerical result. So we select the modified scalar auxiliary variable $R = \exp\left(\frac{\mathcal{E}(\phi)}{C_3}\right)$, where C_3 is enough large positive number (see Example 3).

Theorem 3. *The scheme (45) meets energy dissipation law*

$$R^{n+1} - R^n = -\tau \xi^{n+1} \exp(\mathcal{E}(B_6(\phi^n)))\left(\frac{\delta \mathcal{E}(B_6(\phi^n))}{\delta \phi}, \frac{\delta \mathcal{E}(B_6(\phi^n))}{\delta \phi}\right) \leq 0. \tag{46}$$

Moreover, we have

$$\ln(R^{n+1}) - \ln(R^n) \leq 0. \tag{47}$$

Proof. It is evident that $R^n > 0$ from formula $R = \exp(\mathcal{E}(\phi))$. According to the scheme (45b), we have

$$R^{n+1} = \frac{R^n}{1 + \tau\left(\frac{\delta \mathcal{E}(B_6(\phi^n))}{\delta \phi}, \frac{\delta \mathcal{E}(B_6(\phi^n))}{\delta \phi}\right)} > 0,$$

and $\xi^{n+1} \geq 0$. Thus, formula (46) holds. Formula (47) holds because the natural logarithm function is increasing □

5. Numerical experiments

In this section, we provide numerical examples to illustrate convergence and energy stability of the schemes (4) and (45).

Example 1. We consider convergence orders with GSAV method and ESAV method for the SH equation. Add a function g such that the exact solution of problem (1) is

$$\phi(x, y, t) = \exp(\sin(x)\sin(y))\cos(t),$$

where the domain $[-\pi, \pi]^2$ and $\epsilon = 0.1$.

We use Fourier spectral methods to discretize spatial variables and set 128^2 Fourier modes. In Table 1 and Table 2, we show the errors in the H^2 norm and L^2 norm for GSAV method and ESAV method for the SH equation, respectively. Sixth-order convergence for both methods is verified. When using the ESAV algorithm

TABLE 1. The errors of H^2 norm and L^2 norm (GSAV) for Example 1 with $h = \pi/64$.

τ	$\|\boldsymbol{\phi}^M - \phi^M\|_{H^2}$	Rate	$\|\boldsymbol{\phi}^M - \phi^M\|_{L^2}$	Rate
1/16	5.4347e-007	-	2.7702e-007	-
1/32	7.6237e-009	6.1556	4.1726e-009	6.0529
1/64	1.1351e-010	6.0696	6.2674e-011	6.0569
1/128	2.8470e-012	5.3147	9.4294e-013	6.0546

TABLE 2. The errors of H^2 norm and L^2 norm (ESAV) for Example 1 with $h = \pi/64$.

τ	$\|\boldsymbol{\phi}^M - \phi^M\|_{H^2}$	Rate	$\|\boldsymbol{\phi}^M - \phi^M\|_{L^2}$	Rate
1/16	6.1579e-007	-	3.3809e-007	-
1/32	9.3844e-009	6.0360	5.3102e-009	5.9925
1/64	1.4176e-010	6.0487	8.1464e-011	6.0265
1/128	3.1195e-012	5.5060	1.2325e-012	6.0465

and GSAV algorithm, the error results of H^2 norm and L^2 norm showed similar convergence effect, and with the time step τ, the errors of both algorithms decrease significantly, exhibiting a sixth-order convergence rate.

Example 2. We present numerical simulation results for the classical SH model and choose the initial data

$$\phi(x, y, 0) = 0.1 + 0.02\cos\left(\frac{\pi x}{100}\right)\sin\left(\frac{\pi y}{100}\right) + 0.05\cos\left(\frac{\pi x}{20}\right)\sin\left(\frac{\pi y}{20}\right),$$

where $\epsilon = 0.25$ and the domain is $[0, 100]^2$. By using the sixth-order implicit RK method to solve the numerical solutions for the first five layers, we are able to provide highly accurate initial values for subsequent time steps, thus guaranteeing the stability and reliability of the numerical simulation.

In Figure 1, for the fixed parameter $\beta = 0$, we simultaneously present phase transition process of GSAV method and ESAV method at different time points $t = 0.3, 16, 32, 64$. Likewise, Figure 2 shows the evolution of numerical solutions with parameter $\beta = 1$. It is observed that both methods can effectively simulate the SH equation, and different parameters β lead to different numerical results for the SH equation. Figure 3 presents the modified energy dissipation curves (solid lines) of two BDF6 schemes under different parameters: $\beta = 0, \frac{1}{3}, \frac{1}{2}$ and 1. It can be seen that this curve maintains a high degree of consistency with the reference energy (red dashed lines) of the first-order scheme [14]

$$\frac{\phi^{n+1} - \phi^n}{\tau} = -(1 - \epsilon)\phi^{n+1} - \Delta^2\phi^{n+1} - ((\phi^n)^3 - \beta(\phi^n)^2) - 2\Delta\phi^n.$$

We find that all the energy functional values are non-increasing in time for all time steps tested, for both proposed algorithms, which confirms the proposed schemes have unconditional energy stability, as predicted by Theorems 1 and 3.

Example 3. We examine the phase evolution process of the SH equation from a randomly perturbed unstable state to the steady state with 2D and 3D initial data. For 2D case, the initial solution is $\phi(x, y, 0) = 0.07\text{rand}(x, y)$, where $\text{rand}(x, y)$ is the random number in $(-1, 1)$ and the spatial domain is $(x, y) \in [0, 100]^2$. We employ the scheme (45) and set the scalar variable $R(\phi) = \exp\left(\frac{\mathcal{E}(\phi)}{\mathcal{E}(\phi^0)}\right)$, where $\mathcal{E}(\phi^0)$ denotes the energy value in initial solution. In Figures 4 and 5, we show the

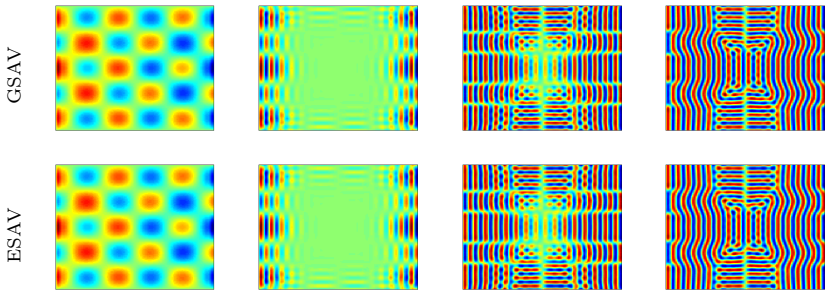

FIGURE 1. Snapshots of GSAV method and ESAV method for $t = 0.3, 16, 32, 64$ with $\beta = 0$.

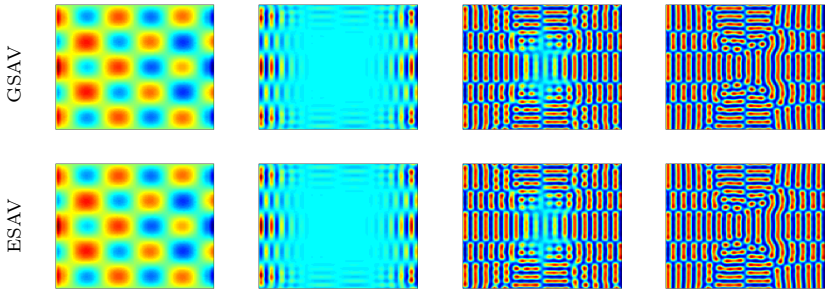

FIGURE 2. Snapshots of GSAV method and ESAV method for $t = 0.3, 16, 32, 64$ with $\beta = 1$.

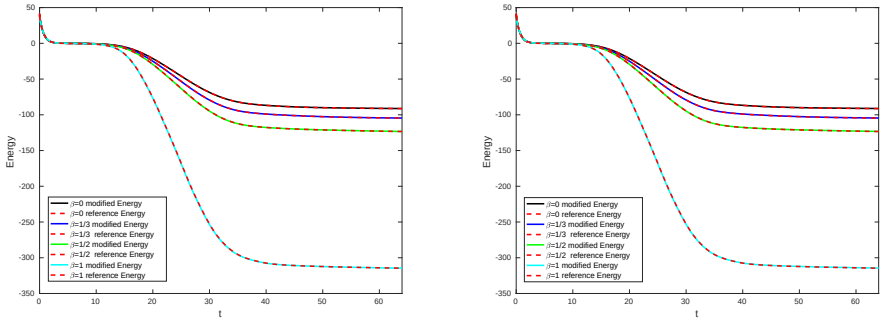

FIGURE 3. Energy values of GSAV method (left) and ESAV method (right) for different $\beta = 0, \frac{1}{3}, \frac{1}{2}, 1$.

phase transition states of scheme (45) with adaptive time stepping ($\tau_{\max} = 10^{-4}$, $\tau_{\min} = 10^{-10}$) and compare them with the first-order scheme employing a fixed time step $\tau = 10^{-4}$, for different β and ϵ. It reaches a steady state as time increases.

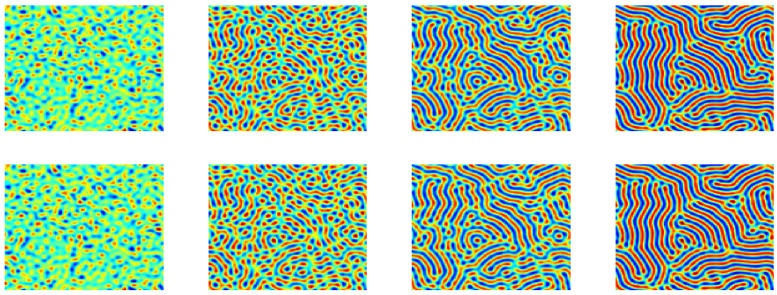

FIGURE 4. Snapshots of ESAV method (First line) and first order convex splitting scheme (Second line) for $t = 1, 20, 40, 100$ when $\epsilon = 0.3, \beta = 0$.

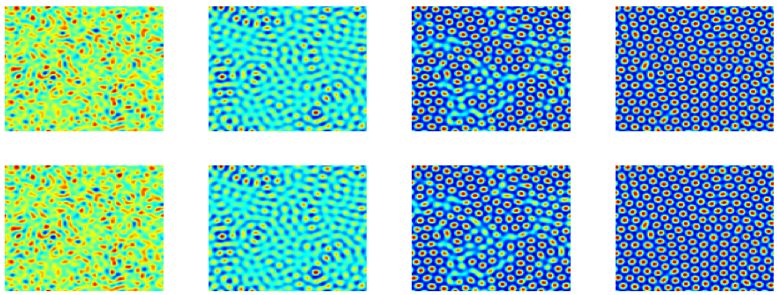

FIGURE 5. Snapshots of ESAV method (First line) and first order convex splitting scheme (Second line) for $t = 1, 20, 40, 100$ when $\epsilon = 0.1, \beta = 1$.

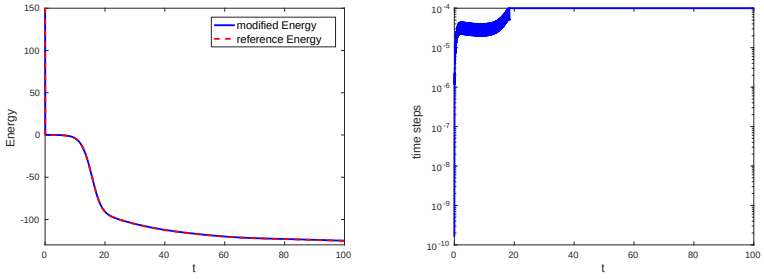

FIGURE 6. Energy values and time step curves of 2D random initial solution ($\epsilon = 0.3, \beta = 0$).

As shown in Figure 6 (left) and 7 (left), by comparing the evolution curves of the modified energy of the BDF6 scheme and the reference energy of the first-order scheme over time, it can be observed that the two remain highly consistent.Meanwhile, Figure 6 (right) and Figure 7 (right) display the time step variation

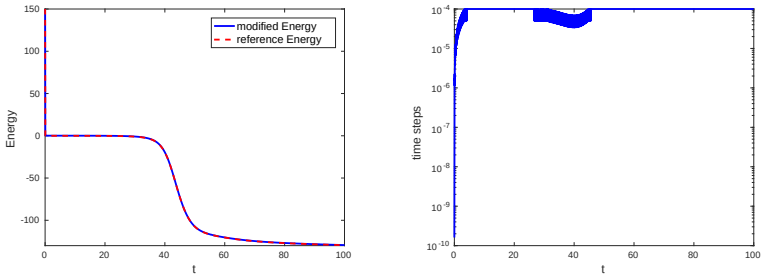

FIGURE 7. Energy values and time step curves of 2D random initial solution ($\epsilon = 0.1, \beta = 1$).

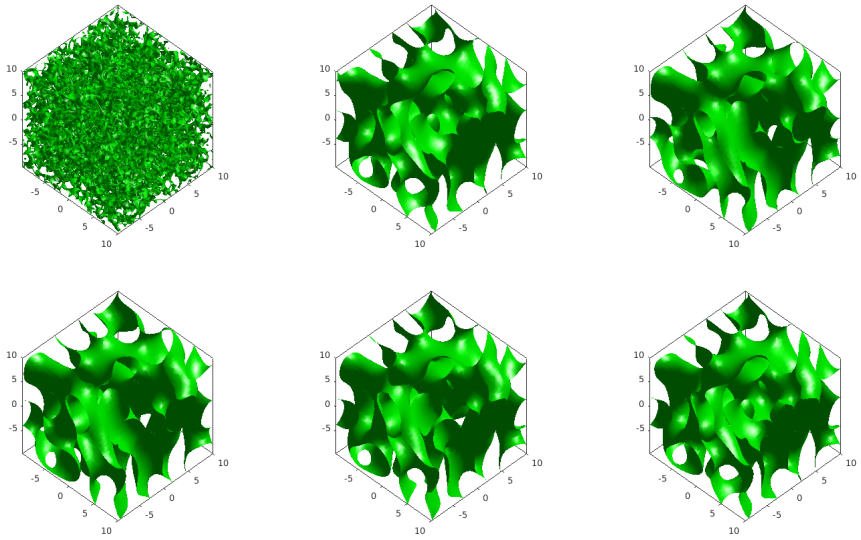

FIGURE 8. Phase-field evolution for time $t = 0, 10, 50, 100, 250, 500$.

graphs. These graphs show that the time steps undergo rapid initial changes, driven by the nonlinear evolution of the phase field model and the algorithm's error control mechanism. Subsequently, the step sizes gradually stabilize, with minor fluctuations reflecting the adaptive strategy's dynamic balance between accuracy and efficiency throughout the simulation.

For 3D case, the initial data is $\phi(x, y, z, 0) = \text{rand}(x, y, z) + 0.5$, where the parameters are $\beta = 1$ and $\epsilon = 0.35$. We use 40^3 spatial modes to discretize the spatial domain $(x, y, z) \in [-10, 10]^3$ and set $C_0 = 400$. In Figure 8, we use adaptive time step (maximum time step $\tau_{\max} = 1e-4$, minimum time step $\tau_{\min} = 1e-10$) to show the states of phase transition in different time t for the scheme (4), which validates that the scheme can lead to the intended state. The adaptive algorithm improves the computational efficiency by dynamically adjusting the calculation grid and time step.

Figure 9 (left) demonstrates excellent agreement between the modified energy and the reference energy curves, confirming the superior stability of the BDF6

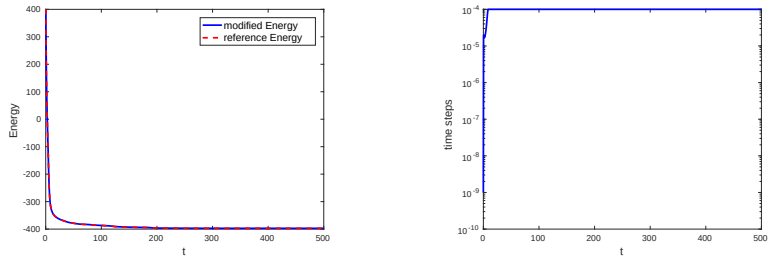

FIGURE 9. Energy values and time step curves of 3D random initial solution ($\epsilon = 0.35, \beta = 1$).

scheme in three-dimensional simulations. The time step curve in Figure 9 (right) exhibits a consistent trend: rapid initial adjustments in response to the phase field's nonlinear dynamics and error constraints, followed by steady stabilization.

6. Conclusion

In this study, we investigate numerical approaches for the SH equation using the BDF6 scheme with GSAV and ESAV methods, and obtain high-order convergence and energy dissipation. The scheme can be extended to AC equations and obeys an energy stability law. However, for the MBE model, CH equation, and PFC model, a complex problem arises: the expression $\Delta B_6(x)$ fails to properly compute the nonlinear term involving the Laplace operator Δ. This will be addressed in future work.

Acknowledgments

This work was supported by the National Natural Science Foundation of China Project (No. 12571469), the Scientific Research Innovation Capability Support Project for Young Faculty of China (No. SRICSPYF-BS2025132), the Project of Scientific Research Fund of the Hunan Provincial Science and Technology Department (No. 2024JJ1008), the 111 Project (No. D23017), the Program for Science and Technology Innovative Research Team in Higher Educational Institutions of Hunan Province of China, and the Hunan Province Postgraduate Research and Innovation Project (CX20230609).

References

[1] Swift, J. and Hohenberg, P., Hydrodynamic fluctuations at the convective instability, Phys. Rev. A, 15: 319-328, 1977.
[2] Wise, S.M., Wang, C. and Lowengrub, J.S., An energy-stable and convergent finite-difference scheme for the phase field crystal equation, SIAM J. Numer. Anal., 47: 2269-2288, 2009.
[3] Anderson, D., Mcfadden, G. and Wheeler, A.A., Diffuse-interface methods in fluid mechanics, Annu. Rev. Fluid Mech., 30: 139-165, 1997.
[4] Chen, L. and Shen, J., Applications of semi-implicit Fourier-spectral method to phase field equations, Comput. Phys. Commun., 108 (2-3): 147-158, 1998.
[5] Su, J., Fang, W., Yu, Q. and Li, Y., Numerical simulation of Swift-Hohenberg equation by the fourth-order compact scheme, Comput. Appl. Math., 38: 54, 2019.
[6] Hutt, A. and Atay, F., Analysis of nonlocal neural fields for both general and gamma-distributed connectivities, Phys. D, 203 (1-2): 30-54, 2005.
[7] Hutt, A., Longtin, A. and Schimansky-Geier, L., Additive noise-induced Turing transitions in spatial systems with application to neural fields and the Swift-Hohenberg equation, Phys. D, 237: 755-773, 2008.

[8] Shen, J. and Huang, F.K., A new class of implicit-explicit BDFk SAV schemes for general dissipative systems and their error analysis, Comput. Methods Appl. Mech. Engrg., 392: 114718, 2022.
[9] Zhang, Y. and Shen, J., A generalized SAV approach with relaxation for dissipative systems, J. Comput. Phys., 464: 111311, 2022.
[10] Zhang, Y. and Li, X., Efficient and accurate exponential SAV algorithems with relaxation for dissipative system, Commun. Nonlinear Sci. Numer. Simul., 127: 107530, 2023.
[11] Shen, J., Xu, J. and Yang, J., The scalar auxiliary variable (SAV) approach for gradient flows, J. Comput. Phys., 353: 407-416, 2018.
[12] Lee, P., A semi-analytical Fourier spectral method for the Swift-Hohenberg equation, Comput. Math. Appl., 74: 1885-1896, 2017.
[13] Akrivis, G., Chen, M., Yu, F. and Zhou, Z., The energy technique for the six-step BDF method, SIAM J. Numer. Anal., 59 (5): 2449-2472, 2021.
[14] Yoon, S., Jeong, D., Lee, C., et., Fourier-Spectral method for the phase-field equations, Mathematics, 8: 1385, 2020.
[15] Lee, H., An efficient and accurate method for the conservative Swift-Hohenberg equation and its numerical implementation, Mathematics, 8 (9): 1502, 2020.
[16] Roger, T., Infinite-dimensional dynamical systems in mechanics and physics, Springer Science & Business Media, 68, 2012.
[17] Qi, L.Z. and Hou, Y., Error analysis of a linear unconditionally energy-stable Leapfrog scheme for the Swift-Hohenberg equation, Commun. Nonlinear Sci. Numer. Simul., 120: 107185, 2023.
[18] Liu, Z.G. and Chen, C.J., On efficient semi-implicit auxiliary variable methods for the six-order Swift-Hohenberg model, J. Comput. Appl. Math., 419: 114730, 2023.
[19] Zhao, X., Yang, R. and Xue, Z.Q., Energy stable and L^2 norm convergent BDF3 scheme for the Swift-Hohenberg equation, arXiv: 2303. 02827, 2023.
[20] Fan, Y. and Chen, M.H., Error analysis of the Crank-Nicolson SAV method for the Allen-Cahn equation on variable grids, Appl. Math. Lett., 125: 107768, 2022.
[21] Yang, J.X. and Kim, J., Linear and energy stable schemes for the Swift-Hohenberg equation with quadratic-cubic nonlinearity based on a modified scalar auxiliary variable approach, J. Eng. Math., 128: 21, 2021.
[22] Zhang, X., Wu, J.W. and Tan, Z.J., Highly efficient, decoupled and unconditionally stable numerical schemes for a modified phase-field crystal model with a strong nonlinear vacancy potential, Comput. Math. Appl., 132: 119-134, 2023.
[23] Liu, N., Qin, H.Y. and Yang, Y., Unconditionally optimal H^1-norm error estimates of a fast and linearized Galerkin method for nonlinear subdiffusion equations, Comput. Math. Appl., 107: 70-81, 2022.
[24] Zhang, B. and Yang, Y., A new linearized maximum principle preserving and energy stability scheme for the space fractional Allen-Cahn equation, Numer. Algorithms, 93: 179-202, 2023.
[25] Zhang, B. and Yang, Y., An adaptive unconditional maximum principle preserving and energy stability scheme for the space fractional Allen-Cahn equation, Comput. Math. Appl., 139: 28-37, 2023.
[26] Yang, J.X., Tan, Z.J. and Kim, J., High-order time-accurate, efficient, and structure-preserving numerical methods for the conservative Swift-Hohenberg model, Comput. Math. Appl., 102: 160-174, 2021.
[27] Gu, X.L., Cai, W.J. and Wang, Y.S., A novel high-order linearly implicit and energy-stable additive Runge-Kutta methods for gradient flow models, arXiv: 2307.03905, 2023.
[28] Gong, Y.Z., Zhao, J. and Wang, Q., Arbitrarily high-order unconditionally energy stable schemes for thermodynamically consistent gradient flow models, SIAM J. Sci. Comput., 42 (1): B135-B156, 2020.
[29] Yu, F. and Chen, M.H., BDF6 SAV schemes for time-fractional Allen-Cahn dissipative systems, arXiv: 2104.09032, 2021.
[30] Akrivis, G., Li, B.Y. and Li, D.F., Energy-decaying extrapolated RK-SAV methods for the Allen-Cahn and Cahn-Hilliard equations, SIAM J. Sci. Comput., 41 (6): A3703-A3727, 2019.
[31] Lee, H.G., An energy stable method for the Swift-Hohenberg equation with quadratic-cubic nonlinearity, Comput. Methods Appl. Mech. Engrg., 343, 40-51, 2019.
[32] Qi, L.Z. and Hou, Y.R., Error analysis of first- and second-order linear, unconditionally energy-stable schemes for the Swift-Hohenberg equation, Comput. Math. Appl., 127: 192-212, 2022.

[33] Yang, Y., Wang, J.D., Chen, Y.P. and Liao, H.L., Compatible L^2 norm convergence of variable-step L1 scheme for the time-fractional MBE model with slope selection, J. Comput. Phys., 467: 111467, 2022.
[34] Qi, L.Z. and Hou, Y.R., An unconditionally energy-stable linear Crank-Nicolson scheme for the Swift-Hohenberg equation, Appl. Numer. Math., 181: 46-58, 2022.
[35] Kang, Y.Y., Liao, H.L. and Wang, J.D., An energy stable linear BDF2 scheme with variable time-steps for the molecular beam epitaxial model without slope selection, Commun. Nonlinear Sci. Numer. Simul., 118: 107047, 2023.
[36] Huang, F.K. and Shen, J., Stability and error analysis of a class of high-order IMEX schemes for Navier-Stokes equations with periodic boundary conditions, SIAM J. Numer. Anal., 59 (6): 2926-2954, 2021.

Hunan Key Laboratory for Computation and Simulation in Science and Engineering, Hunan International Scientific and Technological Innovation Cooperation Base of Computational Science, Xiangtan University, Xiangtan, 411105, Hunan, China.
E-mail: 202231510096@smail.xtu.edu.cn

Key Laboratory of Intelligent Computing and Information Processing of Ministry of Education, Xiangtan University, Xiangtan 411105, Hunan, China.
E-mail: kangyy0101@163.com

Hunan Research Center of the Basic Discipline Fundamental Algorithmic Theory and Novel Computational Methods, Xiangtan University, Xiangtan 411105, Hunan, China.
E-mail: yangyinxtu@xtu.edu.cn